Electronic Supplementary Information for

Acid-base equilibrium dynamics in methanol and dimethyl sulfoxide probed by two-dimensional infrared spectroscopy

Chiho Lee,[†] Hyewon Son,[†] and Sungnam Park[†,§]*

[†]Department of Chemistry, Korea University, Seoul 136-701, Korea.

[§]Multidimensional Spectroscopy Laboratory, Korea Basic Science Institute, Seoul 136-713, Korea

*Authors to whom correspondence should be addressed.

Email addresses: spark8@korea.ac.kr

1. The volume fitting method by using the 2D Gaussian peak functions

The diagonal peaks and cross-peaks in the 2DIR spectrum at a given T_w were successfully fitted by rotated two-dimensional (2D) Gaussian peak functions so that the peak volumes were determined. The rotated 2D Gaussian peak function for each species is given by

$$G(\omega_\tau,\omega_t) = A\cdot\exp\left[-\frac{\left(\omega_\tau-\omega_t-\omega_{\tau 0}+\omega_{t0}\right)^2}{4\sigma_\tau^2}-\frac{\left(\omega_\tau+\omega_t-\omega_{\tau 0}-\omega_{t0}\right)^2}{4\sigma_t^2}\right] - A\cdot\exp\left[-\frac{\left(\omega_\tau-\omega_t+\Delta\omega-\omega_{\tau 0}+\omega_{t0}\right)^2}{4\sigma_\tau^2}-\frac{\left(\omega_\tau+\omega_t-\Delta\omega-\omega_{\tau 0}-\omega_{t0}\right)^2}{4\sigma_t^2}\right], \quad \text{(S1)}$$

where A is the amplitude, $\omega_{\tau 0}$ and ω_{t0} are the peak positions along the ω_τ axis and ω_t axis, σ_τ and σ_t are the diagonal and anti-diagonal widths, respectively, and $\Delta\omega$ is the vibrational anharmonicity. The long axis of the rotated 2D Gaussian peak function is set parallel to the diagonal. The first term in Eq. (S1) represents the 2D Gaussian peak for the v=0→1 transition and the second term is the 2D Gaussian peak for the v=1→2 transition. For the cross-peaks, one parameter (their amplitudes) needs to be determined. For a complete numerical fitting analysis, 13 parameters should be determined. Among them, the peak positions and vibrational anharmonicities can be robustly determined from the 2DIR spectrum. Then, only 7 parameters associated with the peak amplitudes and widths are iteratively varied until the fitted 2DIR spectra converge to the experimental 2DIR spectra. The experimental 2DIR spectra and the fitted 2DIR spectra are compared in Figure S1. The peaks in the 2DIR spectra are well separated and are unambiguously fitted by the 2D Gaussian peak functions.

2. Two-state exchange kinetic analyses for the acid-base equilibrium dynamics

Under thermal equilibrium conditions, as discussed in main text, the acid-base equilibrium dynamics observed in the T_w-dependent 2DIR spectra can be described by the following kinetic scheme,[1-2]

$$\xleftarrow[\text{decay}]{T_1^{A},\tau_{or}^{A}} HN_3 \underset{k_{pro}}{\overset{k_{depro}}{\rightleftharpoons}} H^+ + N_3^- \xrightarrow[\text{decay}]{T_1^{B},\tau_{or}^{B}} \qquad \text{(S2)}$$

where k_{depro} and k_{pro} are the deprotonation and protonation rate constants, respectively, and are related to the acid dissociation constant, $K_a=[H^+][N_3^-]/[HN_3]=k_{depro}/k_{pro}$. Figure S2 illustrates how 2DIR spectrum changes with increasing T_w time based on the two-state exchange kinetic model. As shown in Figure S2, as T_w is increased, two peaks (A and B) associated with acidic (HN_3) and basic (N_3^-) species exchange their populations with the deprotonation and protonation rate constants (k_{depro} and $k'_{pro}=k_{pro}[H^+]$), respectively, and the exchange rate constant is given by $k_{ex}=k_{depro}+k'_{pro}$. T_1^{A} and T_1^{B} are the vibrational lifetimes and τ_{or}^{A} and τ_{or}^{B} are the orientational relaxation times of HN_3 and N_3^-, respectively. In the present work, the activity coefficients of ionic species in solution are ignored. Then, the acid dissociation constant is given by

$$K_a = \frac{[H^+][N_3^-]}{[HN_3]} = \frac{k_{depro}}{k_{pro}} \qquad \text{(S3)}$$

$$K'_a = \frac{[N_3^-]}{[HN_3]} = \frac{k_{depro}}{k'_{pro}} \quad \text{with } k'_{pro} = k_{pro}[H^+] \qquad \text{(S4)}$$

where $[\cdots]$ represents the equilibrium concentration. The time-dependent changes of $[HN_3]$ and $[N_3^-]$ obey the following coupled rate equations,[3]

$$\begin{aligned} \frac{d[HN_3]}{dt} &= -k_{depro}[HN_3] + k'_{pro}[N_3^-] \\ \frac{d[N_3^-]}{dt} &= k_{depro}[HN_3] - k'_{pro}[N_3^-] \end{aligned} \qquad \text{(S5)}$$

where $k'_{pro} = k_{pro}[H^+]$. By using the mass balance, $[N_3^-]_0=[N_3^-]+[HN_3]$, the analytical solutions of the above rate equations are found to be[4-5]

$$
\begin{aligned}
[HN_3]_A(t) &= [HN_3]\frac{k'_{pro} + k_{depro}\exp(-k_{ex}t)}{k_{ex}} \\
[N_3^-]_B(t) &= [N_3^-]\frac{k_{depro} + k'_{pro}\exp(-k_{ex}t)}{k_{ex}} \\
[HN_3]_{B'}(t) &= [HN_3]\frac{k_{depro}\left[1-\exp(-k_{ex}t)\right]}{k_{ex}} \\
[N_3^-]_{A'}(t) &= [N_3^-]\frac{k'_{pro}\left[1-\exp(-k_{ex}t)\right]}{k_{ex}}
\end{aligned}
\tag{S5}
$$

where the exchange rate constant is given by the sum of the deprotonation and protonation constants as $k_{ex}=k_{depro}+k'_{pro}$. In the T_w-dependent 2DIR spectra, $[HN_3]_A(t)$ and $[N_3^-]_B(t)$ are the concentrations associated with the diagonal peaks whereas $[HN_3]_{B'}(t)$ and $[N_3^-]_{A'}(t)$ correspond to the concentrations associated with the cross-peaks. By including the vibrational population relaxation and orientational relaxation process, the analytic expressions for the diagonal and cross-peak amplitudes as a function of T_w are given as[6-7]

$$
\begin{aligned}
I_A(T_w) &= C_A\mu_A^4\left\{\frac{4}{9}e^{-\alpha T_w}\left[\cosh(\beta T_w)-\gamma\sinh(\beta T_w)\right]+\frac{5}{9}e^{-\varphi T_w}\left[\cosh(\xi T_w)-\eta\sinh(\xi T_w)\right]\right\} \\
I_B(T_w) &= C_B\mu_B^4\left\{\frac{4}{9}e^{-\alpha T_w}\left[\cosh(\beta T_w)+\gamma\sinh(\beta T_w)\right]+\frac{5}{9}e^{-\varphi T_w}\left[\cosh(\xi T_w)+\eta\sinh(\xi T_w)\right]\right\} \\
I_{B'}(T_w) &= C_A\mu_A^2\mu_B^2\left\{\frac{4}{9}\frac{k'_{pro}}{\beta}e^{-\alpha T_w}\sinh(\beta T_w)+\frac{5}{9}e^{-\varphi T_w}\frac{k'_{pro}}{\xi}\sinh(\xi T_w)\right\} \\
I_{A'}(T_w) &= C_B\mu_B^2\mu_A^2\left\{\frac{4}{9}\frac{k_{depro}}{\beta}e^{-\alpha T_w}\sinh(\beta T_w)+\frac{5}{9}e^{-\varphi t}\frac{k_{depro}}{\xi}\sinh(\xi T_w)\right\}
\end{aligned}
\tag{S6}
$$

where

$$\alpha = \frac{1}{2}\left(D_A + D_B + k_A + k_B + k'_{pro} + k_{depro}\right)$$

$$\beta = \sqrt{\alpha^2 - \left(D_A D_B + D_B k_A + D_B k'_{pro} + D_A k_B + k_A k_B + k'_{pro}\, k_B + D_A k_{depro} + k_A k_{depro}\right)}$$

$$\gamma = \frac{\alpha - \left(D_{\mathrm{A}} + k_{\mathrm{A}} + k'_{\mathrm{pro}} \right)}{\beta}$$

$$\varphi = \frac{1}{2}\left(k_{\mathrm{A}} + k_{\mathrm{B}} + k'_{\mathrm{pro}} + k_{\mathrm{depro}} \right)$$

$$\xi = \sqrt{\varphi^2 - \left(k_{\mathrm{A}} k_{\mathrm{B}} + k'_{\mathrm{pro}}\, k_{\mathrm{B}} + k_{\mathrm{A}} k_{\mathrm{depro}} \right)}$$

$$\eta = \frac{\varphi - \left(k_{\mathrm{A}} + k'_{\mathrm{pro}} \right)}{\xi}$$

Here, C_α denotes the concentration and μ_α the transition dipole moment. $D_{\mathrm{A}} = 1/\tau_{\mathrm{or}}^{\mathrm{A}}$ and $D_{\mathrm{B}} = 1/\tau_{\mathrm{or}}^{\mathrm{B}}$ are related to the orientational diffusion coefficients, and $k_{\mathrm{A}} = 1/T_1^{\mathrm{A}}$ and $k_{\mathrm{B}} = 1/T_1^{\mathrm{B}}$ are the vibrational population relaxation rates of HN_3 and N_3^-, respectively. For the two-state exchange kinetic analyses, the vibrational lifetimes and orientational relaxation times were directly measured using polarization-controlled IR pump-probe spectroscopy. The concentrations (C_A/C_B) and transition dipole moments (μ_A/μ_B) were determined from the concentration-dependent FTIR spectra as explained in the next section. All known parameters for the kinetic analyses are summarized in Table S1. In the kinetic analyses, only one unknown parameter needs to be independently determined. The kinetic equations in Eq. (S6) were fit to the plots of the peak volumes against T_w time as shown in Figure 2(C) in the main text. Here, the only unknown parameter that should be determined from the kinetic analyses was the deprotonation rate constant, k_{depro}. By using the k_{depro} value, the protonation rate constant ($k'_{\mathrm{pro}}=k_{\mathrm{depro}}/K'_a$) and the exchange rate constant ($k_{\mathrm{ex}}=k_{\mathrm{depro}}+k'_{\mathrm{pro}}$) were readily obtained.

3. Concentration-dependent FTIR spectra and determination of $\varepsilon_{N_3^-} / \varepsilon_{HN_3}$

Figure S2(A) displays the FTIR spectra of HN_3/N_3^- buffers prepared in methanol. First, 0.047g of NaN_3(s) was completely dissolved in methanol to prepare 0.36 M N_3^- solution. Then, different amount of anhydrous sulfuric acid was added. Upon addition of anhydrous sulfuric acid, Na_2SO_4(s) was precipitated because of its low solubility,

$$2NaN_3 + H_2SO_4 \rightarrow 2HN_3 + Na_2SO_4(s)$$

Figure S2(B) shows the decomposition of the FTIR spectrum of an HN_3/N_3^- buffer into two components associated with N_3^- and HN_3 and the areas of two peaks were calculated. From the Beer's law, the absorbance is related to the concentration by $A = \varepsilon bC$. In the low concentration regime, the peak area can be assumed to be directly proportional to the absorbance. The peak areas obtained from the decomposition analysis are plotted against the concentration of N_3^- and HN_3 in Figures S2(C) and S2(D), respectively.

$$A_{N_3^-} = \varepsilon_{N_3^-} bC_{N_3^-} \quad \text{and} \quad A_{HN_3} = \varepsilon_{HN_3} bC_{HN_3}$$

The values of εb for N_3^- and HN_3 were determined by the slope of each plot. Finally, the ratio of extinction coefficients of N_3^- and HN_3 was able to be determined,

$$\frac{\varepsilon_{N_3^-}}{\varepsilon_{HN_3}} = \frac{\left(\mu_{N_3^-}\right)^2}{\left(\mu_{HN_3}\right)^2} = 3.3 \quad \text{or} \quad \frac{\mu_{N_3^-}}{\mu_{HN_3}} = 1.8$$

References

1. Park, K.-H.; Choi, S. R.; Choi, J.-H.; Park, S.; Cho, M. Real-Time Probing of Ion Pairing Dynamics with 2DIR Spectroscopy. *ChemPhysChem* **2010,** *11* (17), 3632-3637.
2. Lee, K.-K.; Park, K.-H.; Kwon, D.; Choi, J.-H.; Son, H.; Park, S.; Cho, M. Ion-pairing dynamics of Li^+ and SCN^- in dimethylformamide solution: Chemical exchange two-dimensional infrared spectroscopy. *J. Chem. Phys.* **2011,** *134* (6), 064506.
3. Son, H.; Nam, D.; Park, S. Real-Time Probing of Hydrogen-Bond Exchange Dynamics in Aqueous NaPF6 Solutions by Two-Dimensional Infrared Spectroscopy. *J. Phys. Chem. B* **2013,** *117*, 13604-13613.
4. Zheng, J.; Kwak, K.; Asbury, J.; Chen, X.; Piletic, I.; Fayer, M. D. Ultrafast solute-solvent complex chemical exchange observed in real time: multidimensional vibrational echo correlation spectroscopy. *Science* **2005,** *309*, 1338-1343.
5. Park, S.; Odelius, M.; Gaffney, K. J. Ultrafast dynamics of hydrogen bond exchange in aqueous ionic solutions. *J. Phys. Chem. B.* **2009,** *113*, 7825-7835
6. Putzer, E. *J. Am. Math. Mon.* **1966,** *73*, 2.
7. Kwak, K.; Zheng, J.; Cang, H.; Fayer, M. D. Ultrafast 2D IR vibrational echo chemical exchange experiments and theory. *J. Phys. Chem. B.* **2006,** *110*, 19998-20013.

Table S1. Parameters used for the two-state exchange kinetic fitting analyses.

	T_1 (ps) [a]	τ_{or} (ps) [b]	μ [c]	Concentration [c]
HN_3	6.0	4.2	1	1
N_3^-	3.0	10.5	1.8	0.42

[a] Average lifetimes obtained by a single exponential function.

[b] Average orientational relaxation times obtained by a single exponential function.

[c] Relative values between two species are used.

Figure S1

(A)

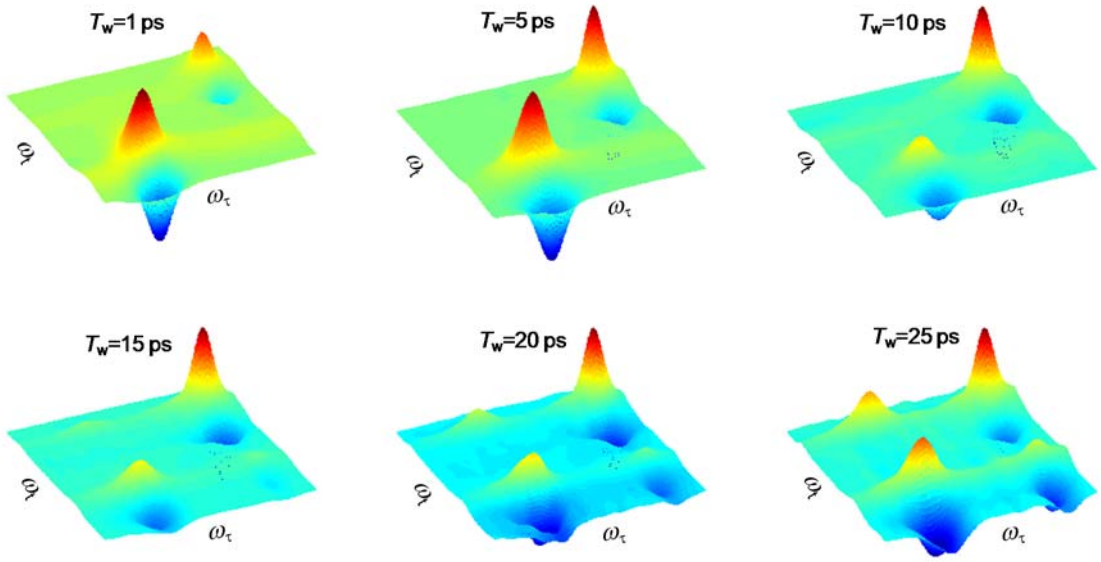

(B)

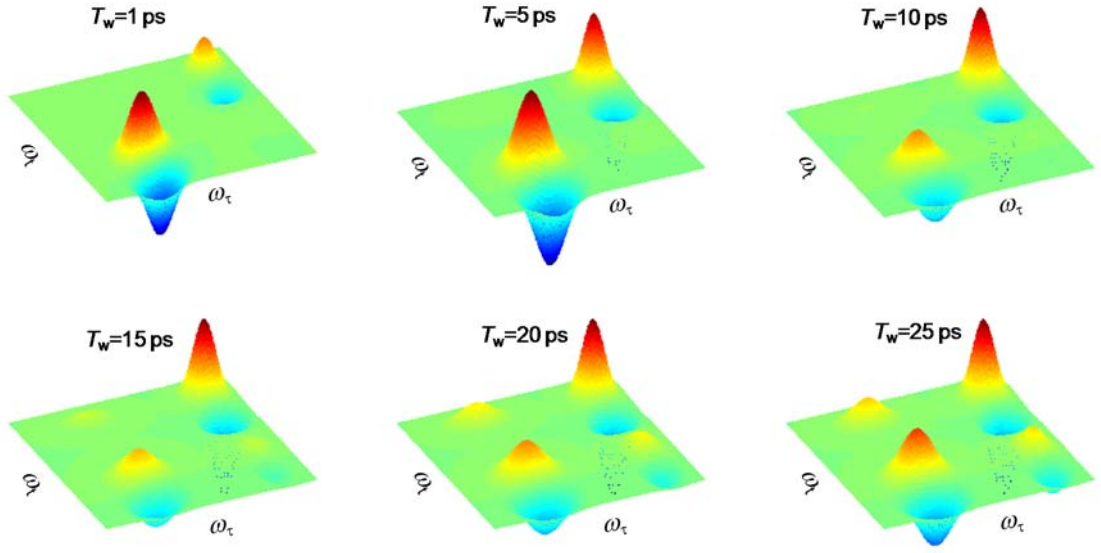

Figure S1. (A) Experimental 2DIR spectra. (B) Fitted 2DIR spectra by 2D Gaussian peak functions.

Figure S2

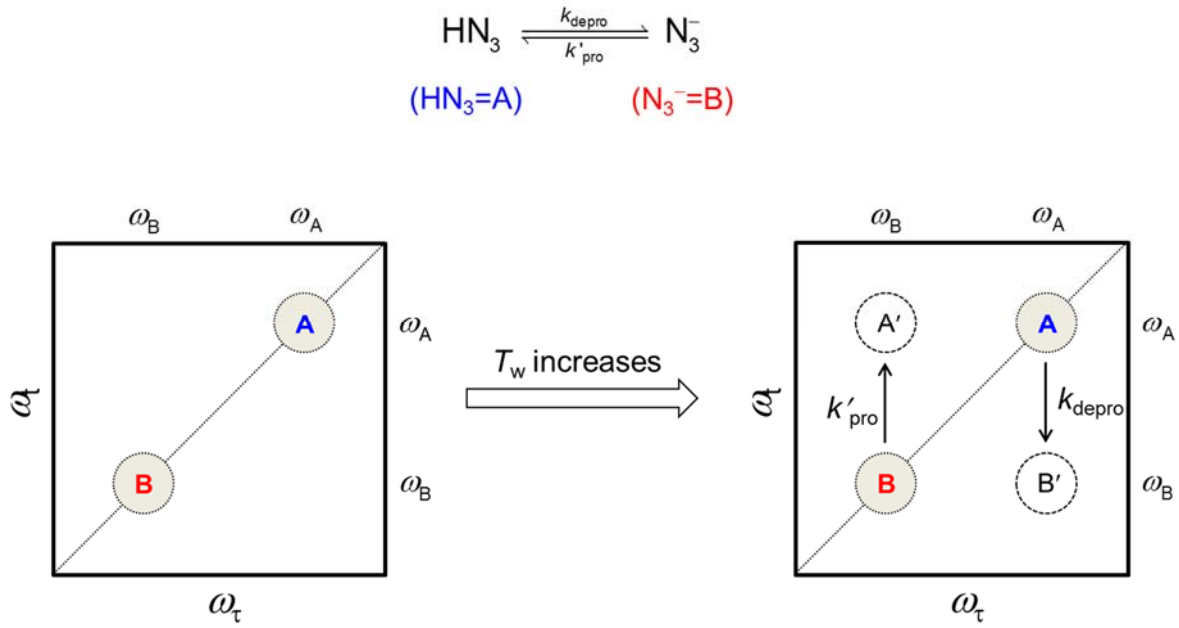

Figure S2. Chemical exchange dynamics observed in the T_w-dependent 2DIR spectra.

Figure S3

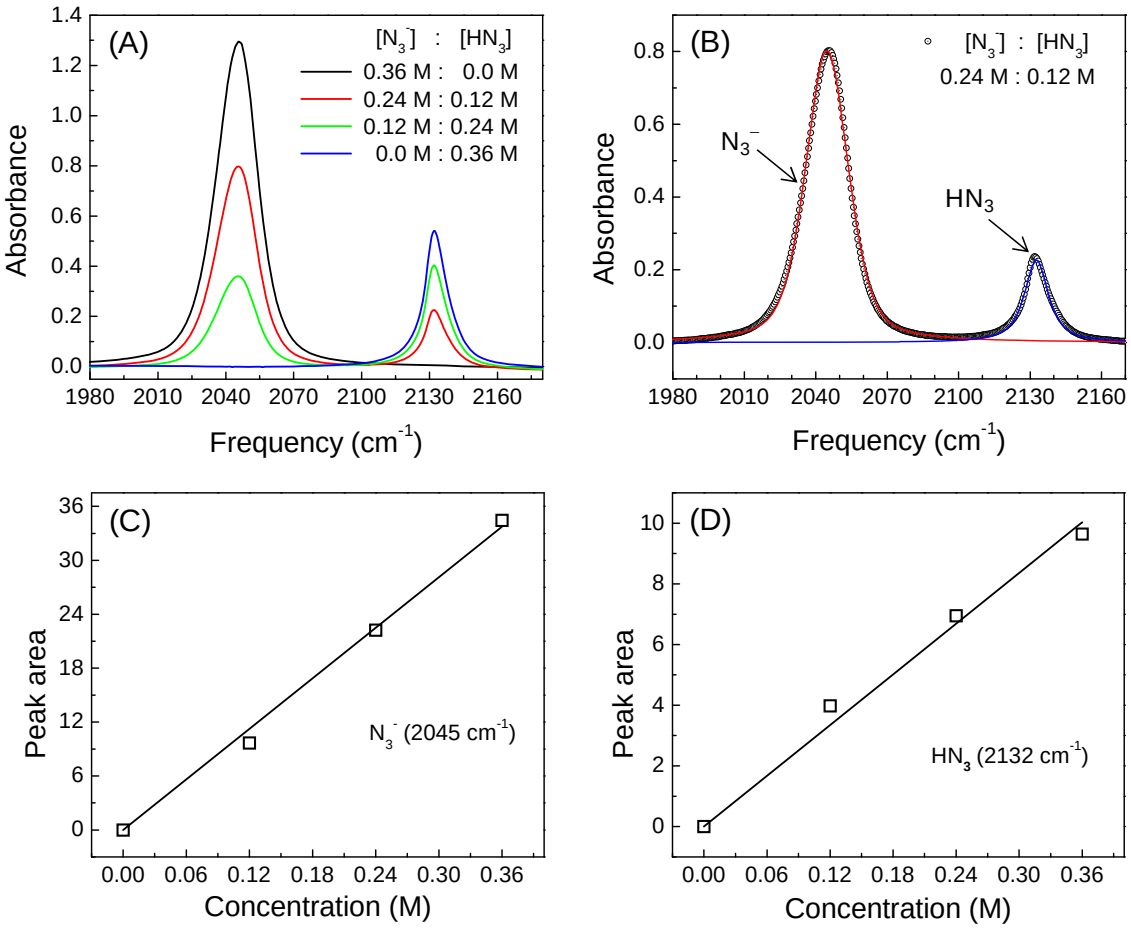

Figure S3. (A) Concentration-dependent FTIR spectra of HN_3/N_3^- buffers in methanol. The cell pathlength was 12 μm. (B) Decomposition of FTIR spectra of an HN_3/N_3^- buffer in methanol. (C) The plot of peak area of N_3^- against concentration. Data points (square) and the linear fit (solid line). (D) The plot of peak area of HN_3 against concentration. Data points (square) and the linear fit (solid line).

Figure S4

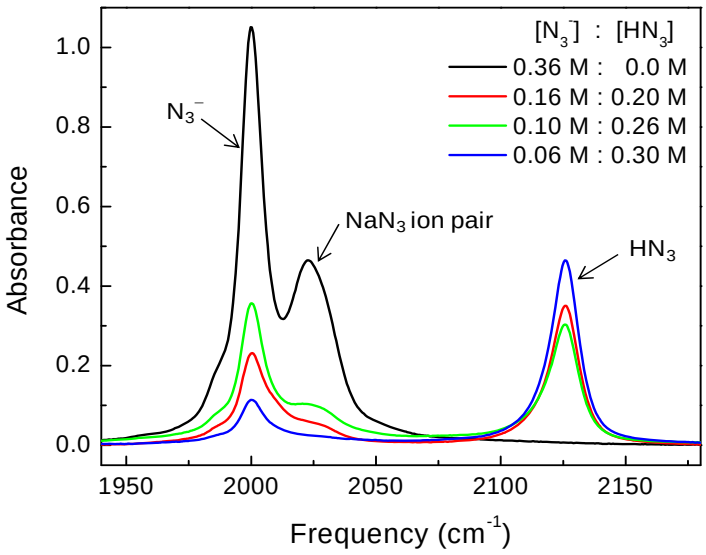

Figure S4. Concentration-dependent FTIR spectra of HN_3/N_3^- buffers in DMSO. The cell pathlength was 12 μm.